

Electronic Supplementary Information (ESI)

Strategic Design of VO₂ encased in N-doped carbon as an efficient electrocatalyst for nitrogen reduction reaction at neutral and acidic media

Ashis Chhetri,^{a,b,§} Ashmita Biswas,^{c,§} Sumana Podder,^{a,b} Ramendra Sundar Dey,^{c,*} Joyee Mitra^{a,b,*}

^a Inorganic Materials & Catalysis Division, CSIR-Central Salt & Marine Chemicals Research Institute, Gijubhai Badheka Marg, Bhavnagar 364002, Gujarat, India.

^b Academy of Scientific and Innovative Research (AcSIR), AcSIR Headquarters, CSIR-HRDC Campus, Sector-19, Kamla Nehru Nagar, Ghaziabad 201002, U.P., India.

^c Institute of Nano Science & Technology, Sector 81, Mohali 140306, Punjab.

Email: joyeemitra@csmcri.res.in, joyeemitra@gmail.com (JM)

rsdey@inst.ac.in (RSD)

§ These authors contributed equally.

Pages: 24 (S1 – S24)

Figures: 20 (S1 – S20)

Index

Sl. No.	Item	Page No.
1	Materials & Methods	S-3
2	Synthesis of VO₂@mel and VO₂@CN	S-3
3	Electrochemical Methods	S-5
4	Characterization data for VO₂@mel	S-9
5	Characterization data for VO₂@CN	S-10
6	FTIR	S-10
7	FT-Raman	S-11
8	TGA	S-12
9	FESEM with EDAX and mapping	S-12
10	SAED pattern of VO₂@CN	S-13
11	Electrochemical cell set-up for NRR	S-13
12	N ₂ gas purity analysis	S-14
13	Potential-dependent chronoamperometric response under various pH	S-15
14	UV-vis spectra at 630 nm, representing different known concentrations of NH ₄ ⁺ stained with indophenol blue indicator solutions	S-16
15	UV-vis spectra at 460 nm, representing different known concentrations of N ₂ H ₄	S-17
16	Comparative bar plot for the Faradaic efficiency of VO₂@CN catalyst at different pH	S-18
17	¹ H-NMR spectra of the electrolytes after NRR performance with VO₂@CN in acid and neutral media	S-19
18	Chronoamperometry and corresponding UV-visible spectra of control samples like VO₂@mel and g-CN compared with VO₂@CN in 0.1 M HCl and 0.1 M Na ₂ SO ₄ respectively	S-20
19	Cyclic voltammetry curves of VO₂@CN in Ar and N ₂ purged acid and neutral electrolytes	S-21
20	Chronoamperometry plots and corresponding UV-visible spectra of VO₂@CN catalyst under N ₂ , Argon and N ₂ under open circuit potential	S-22
21	Post-stability FESEM, TEM and elemental mapping of VO₂@CN sample	S-23
22	XRD spectra of post-electrolysis sample on carbon cloth (CC), compared with fresh VO₂@CN and bare CC	S-24

Materials & Methods

Materials. Melamine, ammonium metavanadate were purchased from Ammonium chloride (NH_4Cl), hydrazine monohydrate ($\text{N}_2\text{H}_4 \cdot \text{H}_2\text{O}$), para-(dimethylamino)benzaldehyde, potassium hydroxide (KOH), sodium hydroxide (NaOH), trisodium citrate, sodium hypochlorite (NaClO), sodium nitroferricyanide ($\text{Na}_2[\text{Fe}(\text{NO})(\text{CN})_5]$), sodium nitrite (NaNO_2), N-(1-naphthyl)- ethylenediamine dihydrochloride, sulfanilic acid and acetic acid were all purchased from Sigma Aldrich. Hydrochloric acid (HCl), sulphuric acid (H_2SO_4), sodium sulphate (Na_2SO_4), phenol, isopropyl alcohol (IPA) and ethanol were purchased from Merck chemicals India. Ti foil was purchased from Goodfellow. All the chemicals used were at least of analytical grade and were used without any further purification. All aqueous solution was prepared using Millipore water.

Synthesis of $\text{VO}_2@\text{mel}$ and $\text{VO}_2@\text{CN}$. 4 gm of melamine was added in a 250 mL round bottom flask containing 50 mL of methanol. The solution was then stirred at room temperature for about 30 minute. 300 mg Vanadium pentoxide dissolved in 20 mL 3M Nitric acid was added to the solution containing melamine under continuous stirring. The reaction mixture was stirred for another one hour at ambient condition. The precipitate was evaporated to dryness.

The obtained $\text{VO}_2(\text{NO}_3)@\text{melamine}$ (referred to as $\text{VO}_2@\text{mel}$) was transferred into an alumina boat placed inside a tubular furnace and heated to 600 °C under continuous nitrogen flow for 3 hrs to obtain a dark grey powder named as $\text{VO}_2@\text{CN}$.

Ex-situ material characterizations. AR grade chemicals were purchased from commercial sources and used without any further purification. The powder X-ray diffraction (PXRD) analysis was done using Philips X'pert MPD system (PANalytical diffractometer) with Cu $\text{K}\alpha 1$ radiation ($\lambda = 0.154 \text{ nm}$). The diffraction pattern was measured in the 2θ range from 5-80° at an operating voltage of 40 kV, 30 mA current, with a scan speed of 3° min⁻¹ and a step size of

0.013° in 2θ at RT with a scan step time 58.395 sec. Anode material was Cu and the value of $K_{\alpha 1}$, $K_{\alpha 2}$ and K_{β} were 1.54060 [Å], 1.54443 [Å] and 1.39225 [Å] respectively. Fourier transform Infrared Spectra analysis (FT-IR) was recorded on Perkin Elmer-Spectrum G-FTIR spectrometer (Germany) from 400-4000 cm^{-1} with a resolution of 4 cm^{-1} using KBr pellets. The FT-Raman spectra were collected on a LabRAM HR Evolution Raman Spectrometer with a 532 nm laser source. The surface morphology of prepared gel material was analyzed by Field Emission- Scanning Electron Microscope (FE-SEM) (JEOL JSM 7100F) with an accelerating voltage of 5–15 kV with 10 μA of emission current. The transition electron microscope (TEM) analysis was done with JEOL, JEM 2100 TEM instrument. XPS analysis was recorded with Omicron ESCA (Oxford Instruments, Germany) instruments. The surface elemental composition and bonding configuration of the prepared samples was determined using X-ray photoelectron spectroscopy (XPS) spectrometer (K-Alpha 1063) instruments in an ultrahigh vacuum chamber (7×10^{-9} torr) using Al-K_{α} radiation (1486.6 eV). UV-vis characterizations were performed in UV-vis-NIR (Cary 5000 UV-vis-NIR, Model: G9825A CARY) spectrophotometer that has the ability to measure 300–2800 nm by a Pb Smart NIR detector. A more precise analysis of the produced ammonia was determined with ^1H nuclear magnetic resonance (NMR) measurements in a 400 MHz Bruker Avance II 400 NMR spectrometer. All the pH measurements were done using Eutech pH meter instrument. All the electrochemical measurements were performed in CHI 760E and BioLogic VSP potentiostats. The in-situ Fourier transform infra-red (FTIR) spectroscopy was performed in ATR mode with 128 scans and 4 resolution on a Bruker Alpha FTIR spectrometer in the range from 500 to 4000 cm^{-1} at room temperature.

Electrode modification. A quantitative amount of $\text{VO}_2@\text{CN}$ catalyst was dispersed in a 1:1 (v/v) mixture of water and isopropyl alcohol (1 mL) and ultrasonicated for 30 minutes. This same ink solution was used for all the electrochemical studies involved in NRR. The Ti foil

(1×1 cm²) used as a substrate was pre-treated with 6 M HCl followed by DI water and IPA before modifying it with 0.5 mg cm⁻¹ catalyst ink.

Electrochemical methods. All the electrochemical measurements were accomplished in an H-type electrolysis cell where the cathode and anode compartments were separated by Nafion (115) membrane allowing proton permeability across it. The Nafion membrane was precleaned in 5 wt% H₂O₂ aqueous solution at 80 °C for 1 h followed by rinsing in ultrapure water at 80 °C for next 1 h. All the measurements were ambiently performed at room temperature in a conventional three-electrode condition with Pt wire, Ag/AgCl (3 M KCl) and VO₂@CN modified Ti foil taken as the counter, reference and working electrodes respectively. All potentials reported in this work were calibrated with respect to the reversible hydrogen electrode (RHE) by the formula given in equation 1 as follows:

$$E_{\text{RHE}} = E_{\text{Ag/AgCl}} + (0.0591 \times \text{pH}) + 0.210 \text{ (E}^0 \text{ at Ag/AgCl, 3 M KCl)} \quad (1)$$

Prior to each electrolysis, the electrolyte in the cathode compartment was continuously fed with pure Ar and N₂ (99.99 % purity) gases for 30 min using properly positioned spargers so as to saturate the catholyte with the desired feed gas. In order to surpass the possibilities of N-contaminations from the N₂ gas, it was trapped in acid and base solutions before using for the electrocatalytic characterizations concerning NRR. All the polarization curves were steady-state ones after 10 cycles and were measured at 10 mV s⁻¹ scan rate and the reported current density values were area-normalized. Chronoamperometric (CA) tests were conducted in the N₂-fed electrolyte solutions for 1 h over the potential range from 0.0 V to – 0.4 V vs RHE. After each CA tests, measured amount of aliquot was taken out from the electrolyte and studied by Indophenol blue and Watt and Chrisp methods for the qualitative detection of ammonia and hydrazine respectively.

N₂ gas purification. The ¹⁴N₂ gas, commercially purchased from Sigma Aldrich (99.99 % pure) was successively passed through acid (0.05 M H₂SO₄) and alkaline (0.1 M KOH) traps to remove the possible nitrogenous contaminants. The trap solutions were further subjected to colorimetric detection techniques to verify the presence of trapped NH₄⁺ or NO_x. All the electrochemical characterizations were performed with the pure feed gas, after being passed through traps.

Determination of NO_x contamination in feeding gas and all the working electrolytes. NO_x in the base trap was determined with the N-(-1-naphthyl)- ethylenediamine dihydrochloride spectrophotometric method. The chromogenic agent was obtained by dissolving sulfanilic acid (0.5 g) in deionized water (90 ml) and acetic acid (5 ml), followed by adding N-(1-naphthyl)- ethylenediamine dihydrochloride (5 mg) and bringing the solution to 100 ml. The prepared solution was incubated in dark. The chromogenic agent (4 mL) was mixed with 1 mL of the investigating solutions. After standing in darkness for another 15 min, the absorption spectrum was measured using an ultraviolet-visible spectrophotometer at 546 nm.

Detection methods of ammonia and hydrazine. Ammonia was detected following the conventional Indophenol Blue method with slight modifications. 5 mL of the aliquot solution was taken and added to 2 mL of 10 mg mL⁻¹ phenol solution in ethanol, followed by 0.2 mL of 0.5 wt% of C₅FeN₆Na₂O (sodium nitroferricyanide) in water. The resulting solution was added with NaOH solution containing trisodium citrate as buffer, till the pH reached above 9. Finally, 0.1 mL of NaClO was added and the solution mixture was stored in dark for 2 h before UV-visible spectroscopic analysis at ~ 630 nm. The concentration of ammonia evolved in the reduction process was determined by a calibration plot (concentration vs absorbance) obtained from a set of solutions containing a known concentration of NH₄Cl in both 0.1 M Na₂SO₄ and 0.1 M HCl. To each of these solutions, the above-mentioned reagents were added and their absorbance was measured after a 2 h incubation time.

For hydrazine detection, the indicator solution contained 0.6 g of para-(dimethylamino) benzaldehyde in 30 mL absolute ethanol and 3 mL concentrated HCl (35%). 2 mL of this color agent was mixed to same volume of the electrolyte solution and incubated in dark for 15 minutes before performing the UV-visible spectroscopic characterization. A set of solutions with known concentration of N₂H₄ in 0.1 M Na₂SO₄ and 0.1 M HCl was used as a calibration standard and their absorbance was measured at $\lambda = 460$ nm.

Activity descriptors. The NH₃ yield rate (R_{NH_3}), normalized to mass, given by mol h⁻¹ mg_{cat}⁻¹ can be calculated using Equation 2, where C is the measured NH₃ concentration (μg mL⁻¹), V is the volume of the catholyte (mL), t is the electrolysis time (h), M is the relative molar mass of NH₃ (M = 17 g mol⁻¹) and mg_{cat} is the mass of the catalyst loaded on the electrode surface.

$$R = \frac{C \times V}{M \times t \times mg_{cat}} \quad (2)$$

The Faradaic efficiency (FE) is calculated using Equation 3, where 3 is the number of electrons necessary to produce one NH₃ molecule, F is the Faraday constant (96485 C mol⁻¹), M is the relative molar mass of NH₃ (M = 17 g mol⁻¹), and the Q is the total charge passed through the electrodes (C).

$$FE = \frac{3 \times F \times C \times V}{M \times Q}$$

¹H NMR studies. NMR measurements were carried out with DMSO-*d*₆ as solvent. Prior to NMR sample preparation, the electrolyte solution was concentrated to 1 mL and a quantitative amount of the sample was added to DMSO-*d*₆ and subjected to 3000 scans for getting a proper triplet signal (with coupling constant $j=52$ Hz) for ¹⁴NH₄⁺. It is to be noted that, the coupling constant values are calculated as a product of the chemical shift value (δ in ppm) and 400 MHz (spectrometer frequency) using equation 3.

$$\delta(ppm) = j(Hz)/spectrometer\ frequency\ (MHz)$$

(3)

Quantification of NH₃ Concentration from NMR. The catholyte solution was concentrated to 1 mL and was taken for NMR analysis. This was subsequently added with 0.01 M maleic acid solution followed by DMSO-*d*₆ and subjected to ¹H-NMR study. The obtained peaks were integrated and by using the following equation 4, the concentration of NH₃ was quantified and matched with that obtained from UV–visible spectroscopic method.

$$(I_{sample})/(I_{standard}) = (H_{sample} \times C_{sample})/(H_{standard} \times C_{standard}) \quad (4)$$

where I stands for the integral values, H stands for the number of protons (4 in case of sample NH₄⁺ and 2 in case of the vinylic protons of maleic acid) and C stands for the concentrations of the sample and standard (0.01 M for maleic acid).

Characterization data of VO₂@mel

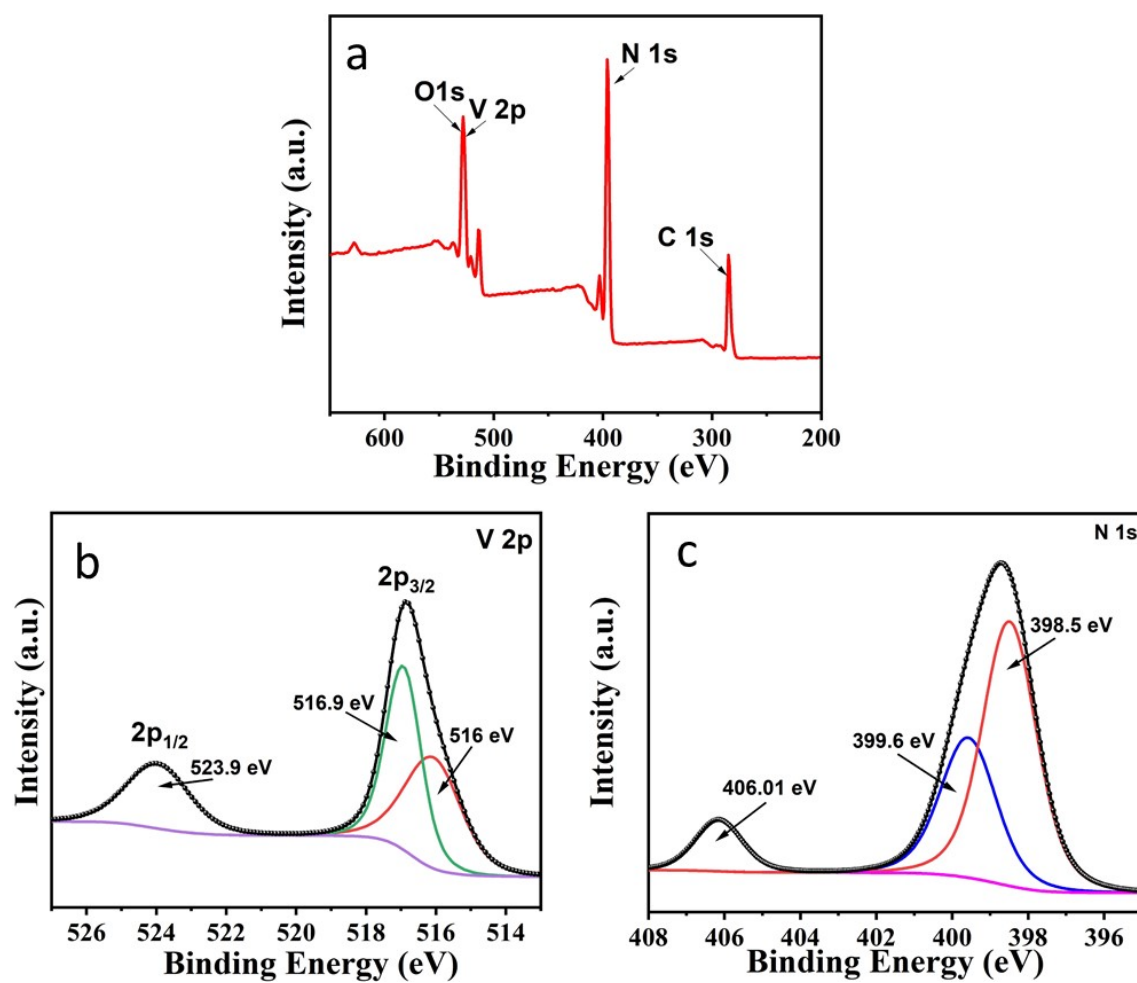


Figure S1. a) XPS survey spectrum, b) V 2p spectrum and c) N 1 s spectrum of VO₂@mel.

Characterization data of VO₂@CN

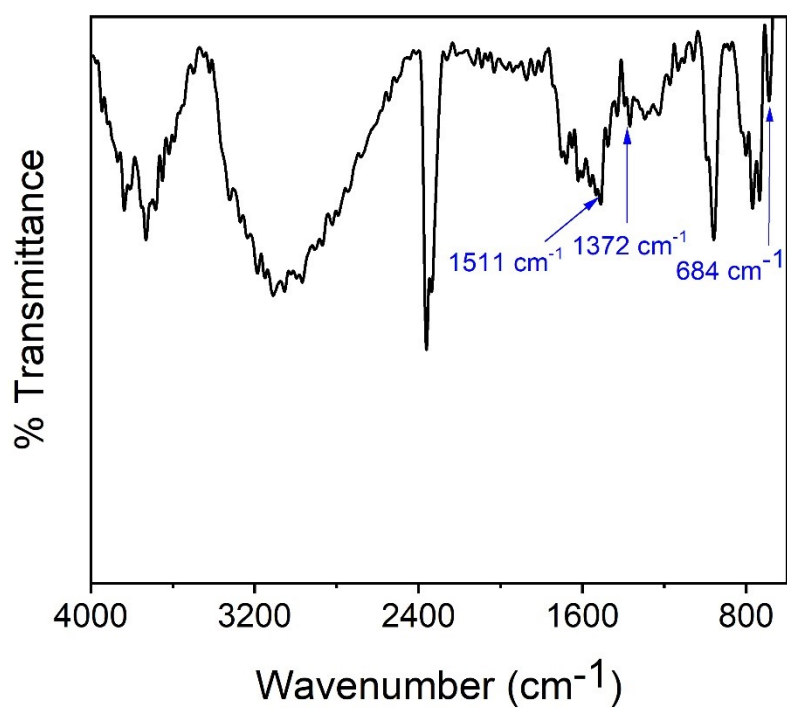


Figure S2. FTIR of VO₂@CN.

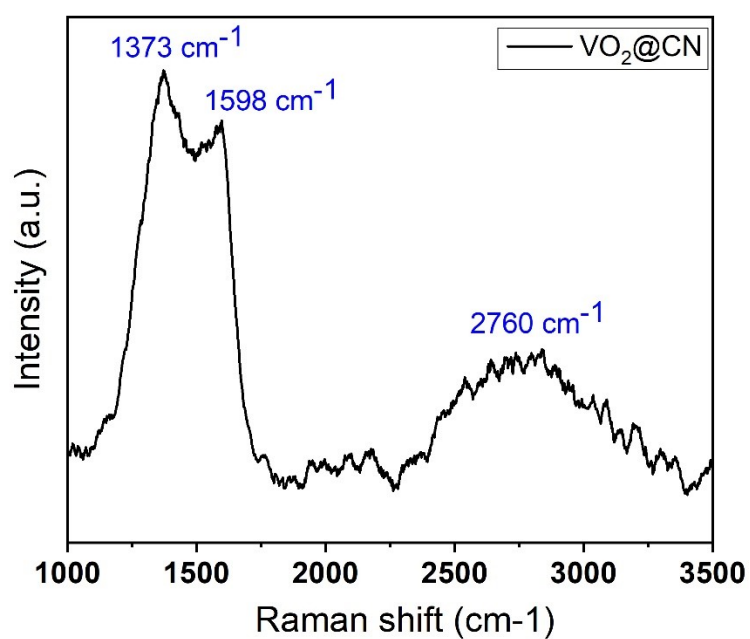


Figure S3. Raman spectrum of VO₂@CN.

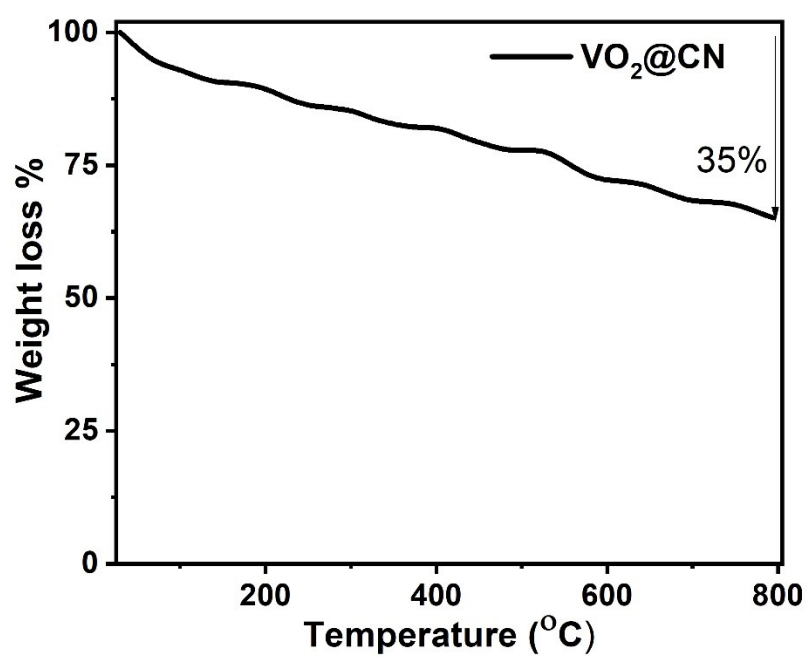


Figure S4. TGA measurements of VO₂@CN.

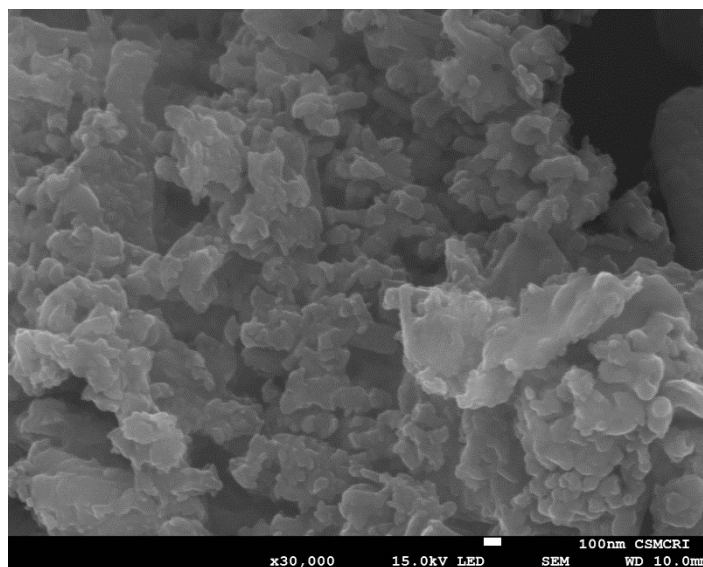


Figure S5. FESEM image of pristine N-doped carbon (g-CN).

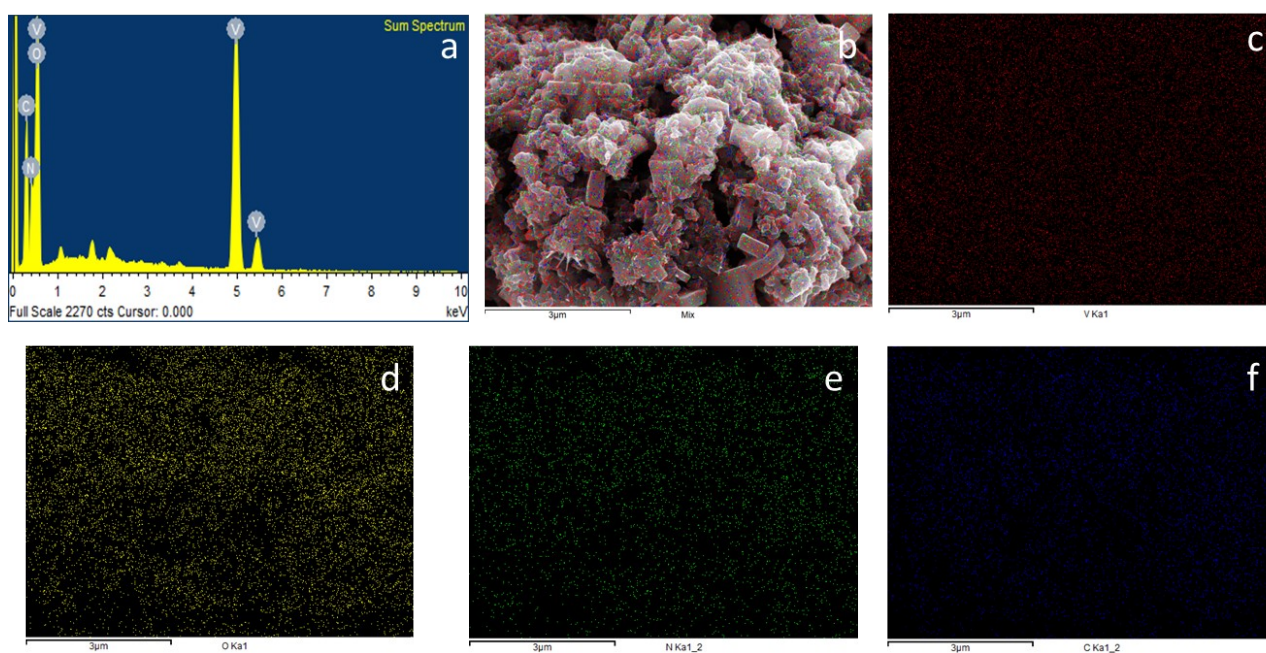


Figure S6. EDAX and Elemental mapping depicting the presence of elements V, O, C and N in $\text{VO}_2@\text{CN}$.

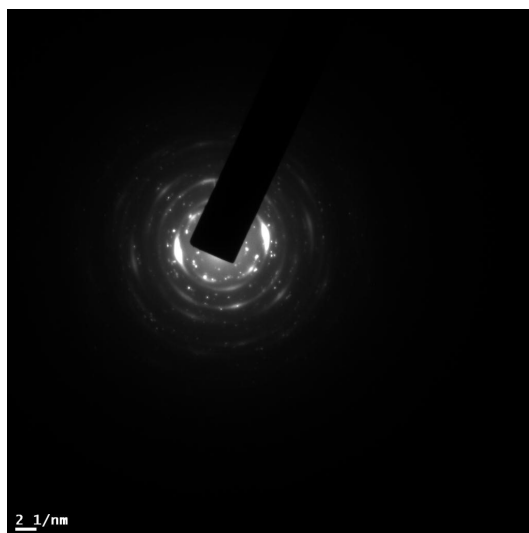


Figure S7. SAED pattern of VO₂@CN.

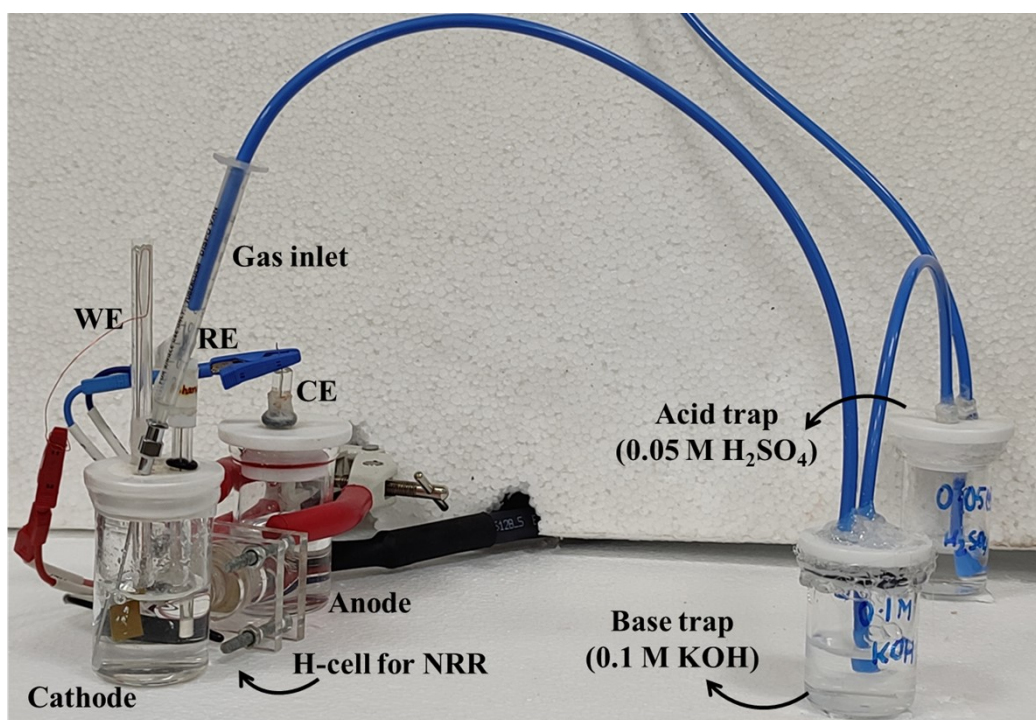


Figure S8. Electrochemical cell set-up for NRR.

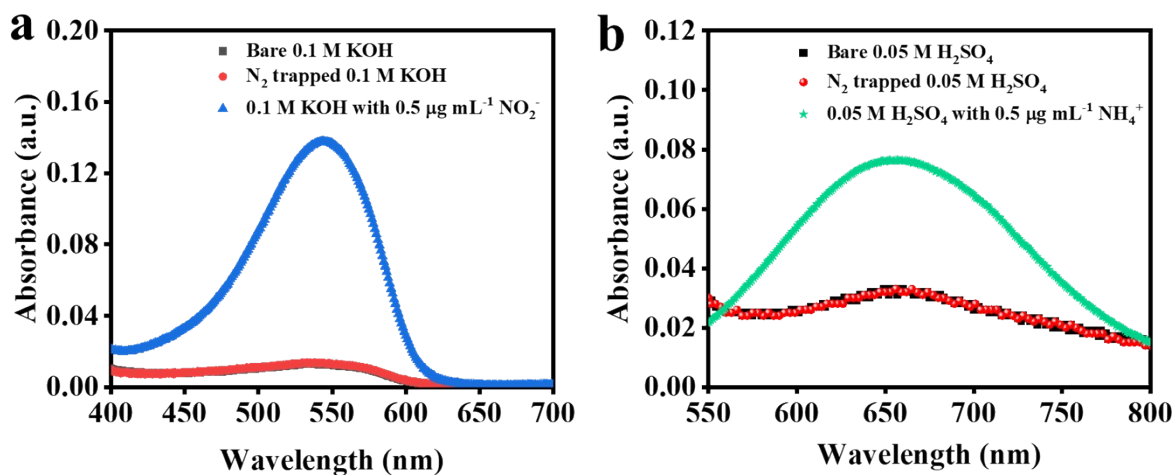


Figure S9. $^{14}\text{N}_2$ gas purity analysis. (a) Spectroscopic analysis for the detection of NO_x dissolved in the 0.1 M KOH trap solution; (b) Indophenol spectrophotometric analysis of ammonia dissolved in 0.05 M H_2SO_4 . Blank data were obtained for the freshly prepared solutions and compared with that containing $0.5 \mu\text{g mL}^{-1}$ of NO_2^- and NH_4^+ respectively.

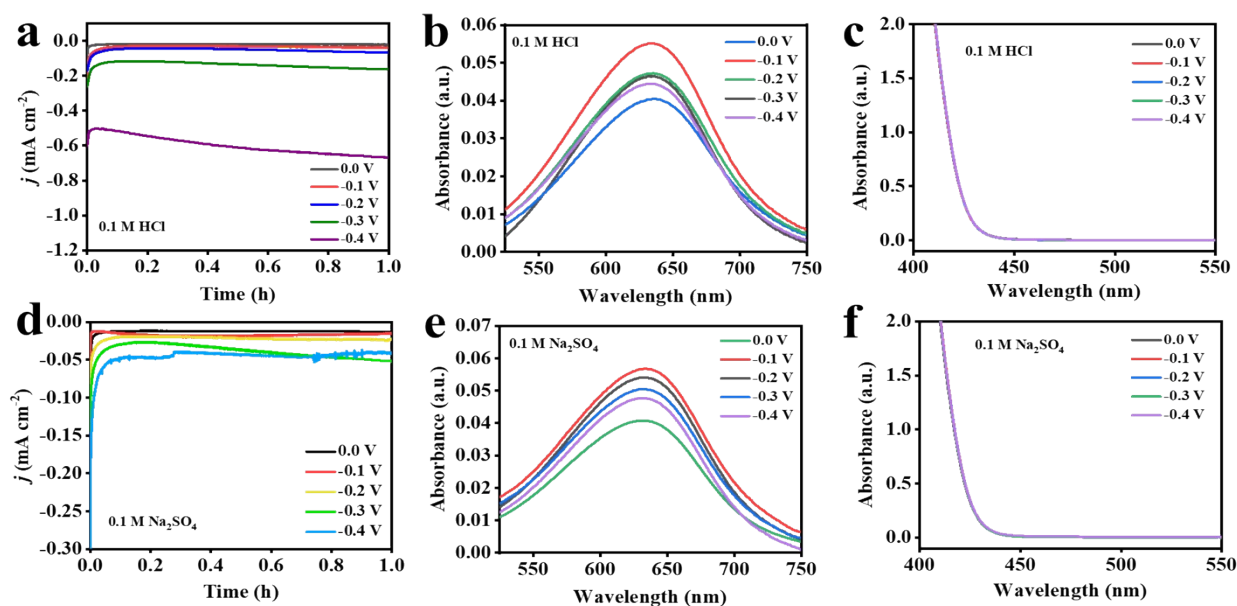


Figure S10. (a) Potential dependent CA response of $\text{VO}_2@\text{CN}$ catalyst for 1 h run (each) in 0.1 M HCl electrolyte; corresponding UV-vis absorption spectra of the electrolyte after each chronoamperometric run (b) stained with indophenol blue indicator for ammonia detection after 2 h incubation period and (c) stained with Watt and Chrisp reagents for the detection of hydrazine after 15 min of incubation from the chronoamperometric run; (d) Potential dependent CA response of $\text{VO}_2@\text{CN}$ catalyst for 1 h run (each) in 0.1 M Na_2SO_4 electrolyte; corresponding UV-vis absorption spectra of the electrolyte after each chronoamperometric run (e) stained with indophenol blue indicator for ammonia detection after 2 h incubation period and (f) stained with Watt and Chrisp reagents for the detection of hydrazine after 15 min of incubation from the chronoamperometric run.

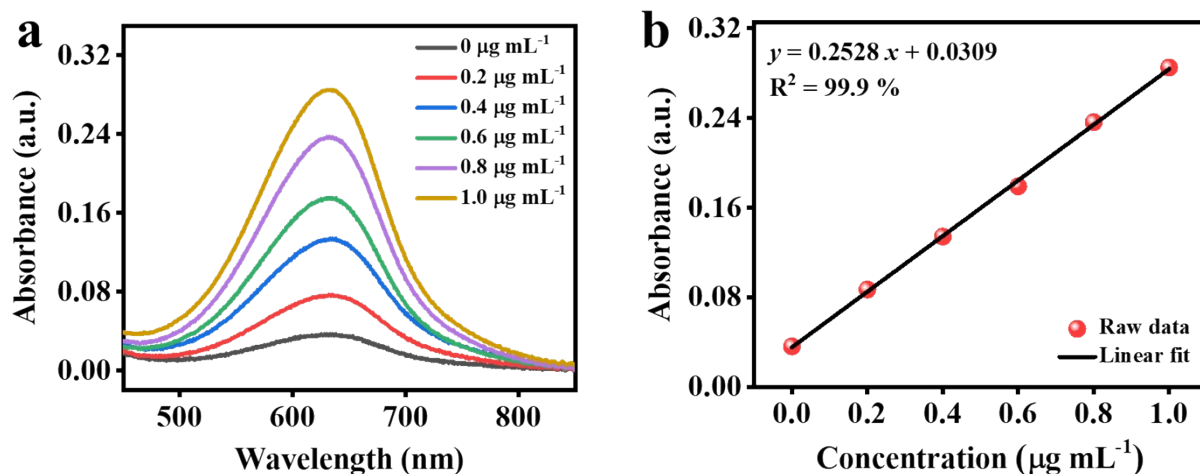


Figure S11. (a) UV-vis spectra at 630 nm, representing different known concentrations of NH_4^+ stained with indophenol blue indicator solutions after 2 h incubation at room temperature in 0.1 M HCl. (b) corresponding linear fit for the absorbance vs concentration plot used in this study.

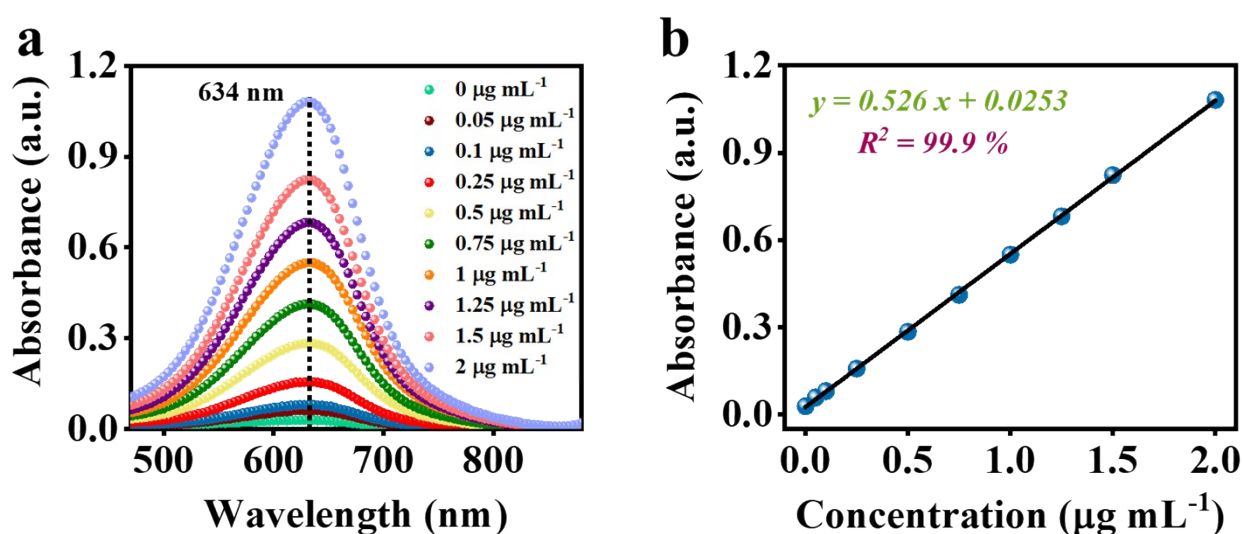


Figure S12. (a) UV-vis spectra at 634 nm, representing different known concentrations of NH_4^+ stained with indophenol blue indicator solutions after 2 h incubation at room temperature in 0.1 M Na_2SO_4 . (b) corresponding linear fit for the absorbance vs concentration plot used in this study.

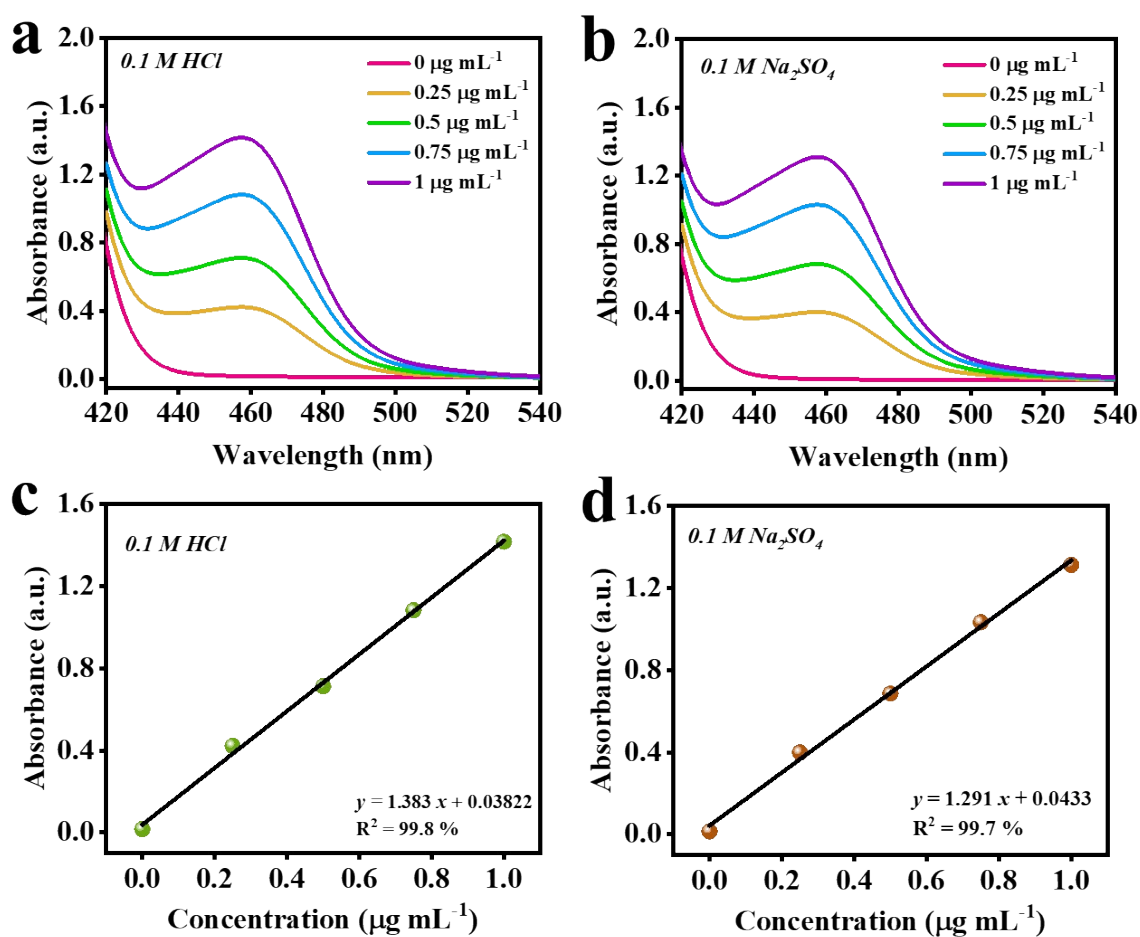


Figure S13. UV-vis spectra at 460 nm, representing different known concentrations of N_2H_4 after 15 min incubation at room temperature in (a) 0.1 M HCl and (b) 0.1 M Na_2SO_4 ; (c, d) corresponding absorbance calibration plot used in this study.

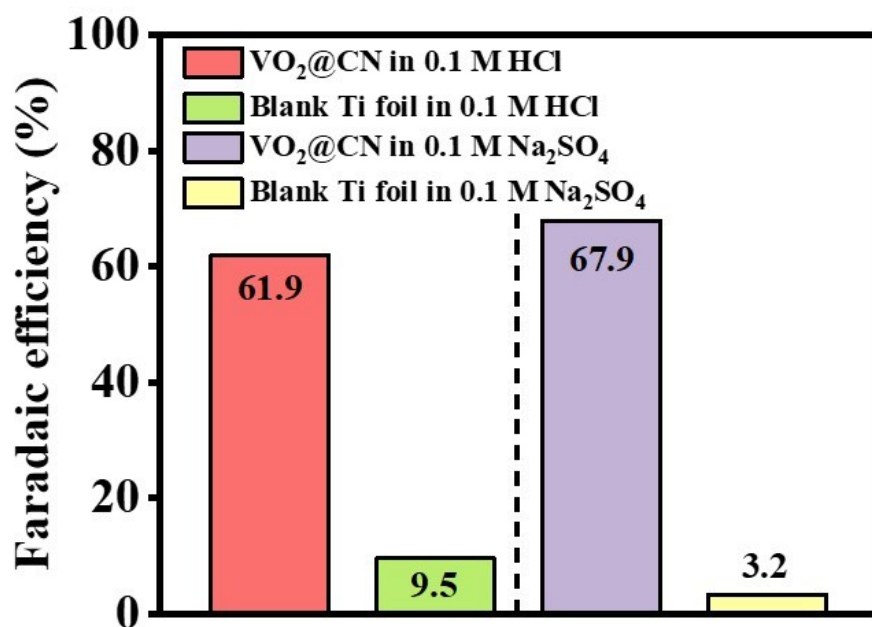


Figure S14. Comparative bar plot for the Faradaic efficiency of $\text{VO}_2@\text{CN}$ catalyst and blank Ti foil in 0.1 M HCl and 0.1 M Na_2SO_4 electrolytes in N_2 purged condition after 1 h chronoamperometry at -0.1 V.

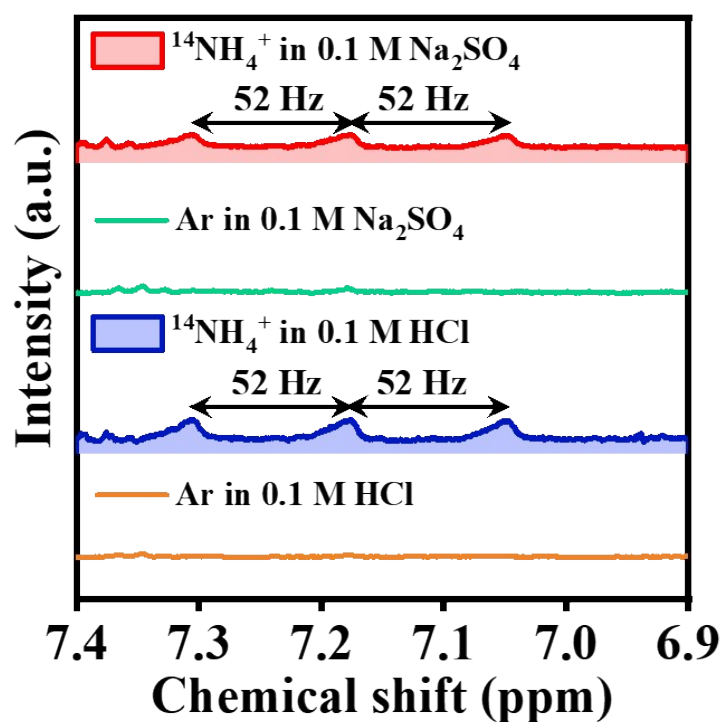


Figure S15. ^1H -NMR spectra of the concentrated electrolyte solutions after NRR experiments in Ar and N_2 purged 0.1 M Na_2SO_4 and 0.1 M HCl respectively showing no peak in Ar and triplets in N_2 condition.

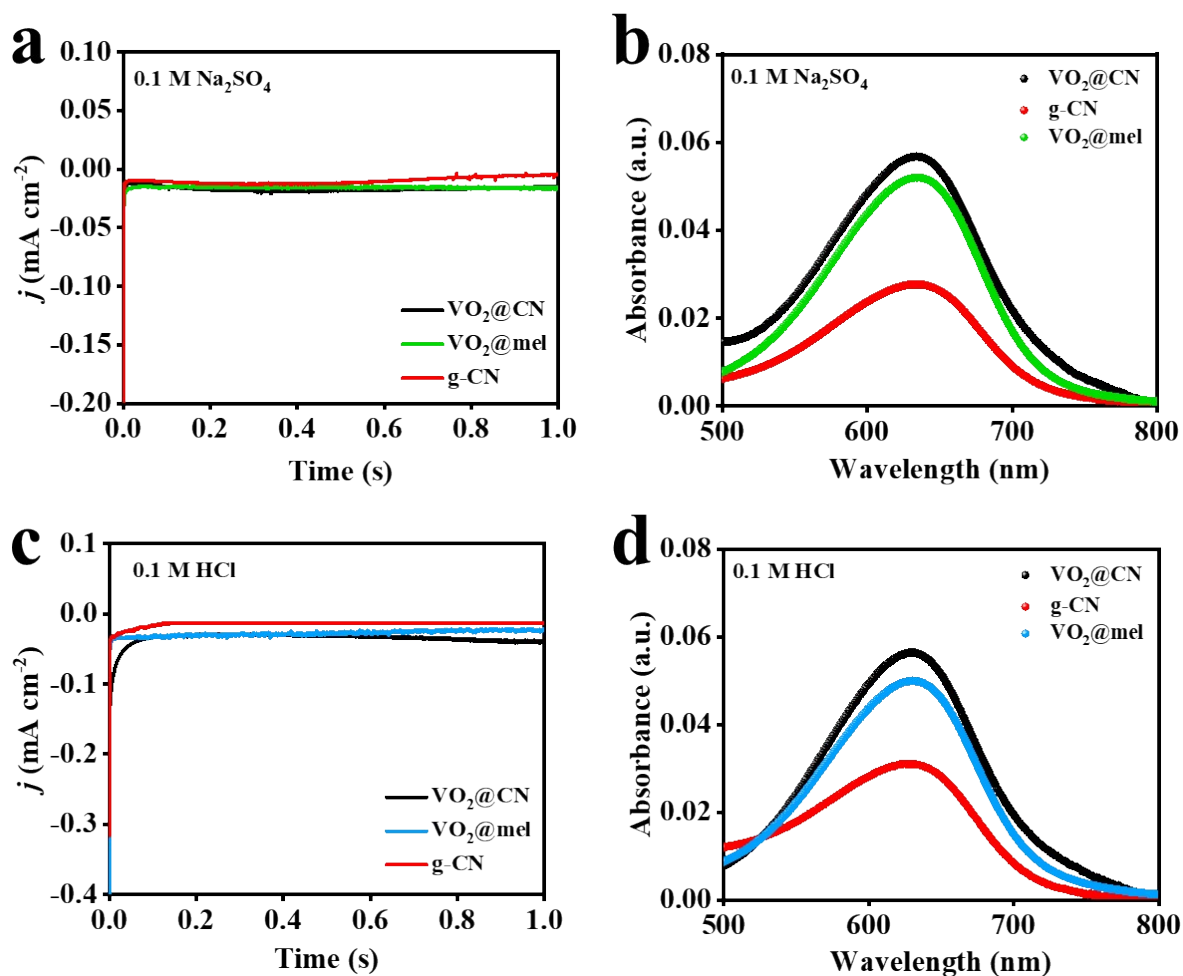


Figure S16. CA responses of the control samples like $\text{VO}_2@\text{mel}$ and g-CN compared with $\text{VO}_2@\text{CN}$ in (a) 0.1 M Na_2SO_4 and (c) 0.1 M HCl and the corresponding UV-visible spectra of the electrolytes ((b) 0.1 M Na_2SO_4 and (d) 0.1 M HCl) after 2 h of incubation time, stained with Indophenol blue indicators.

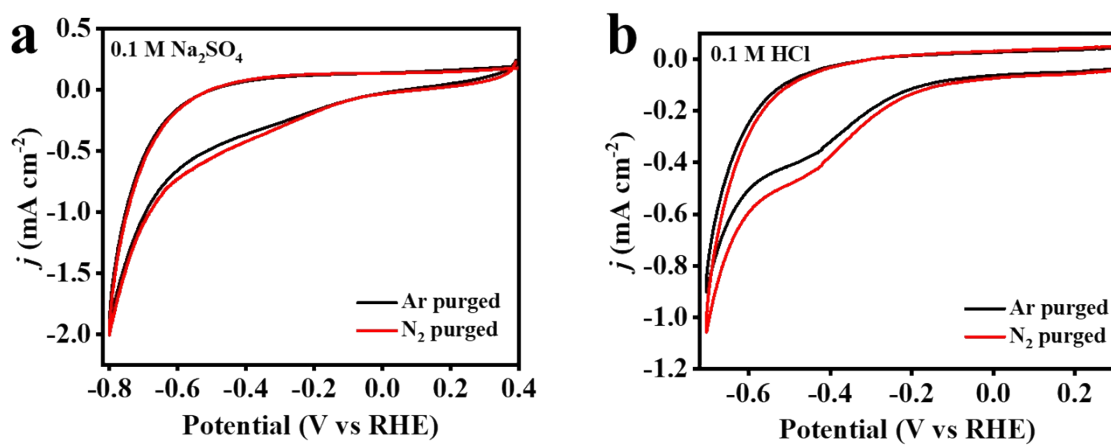


Figure S17. (a, b) Cyclic voltammetry curves of the VO₂@CN catalyst in Ar and N₂ purged electrolyte conditions at 10 mV s⁻¹ scan rate.

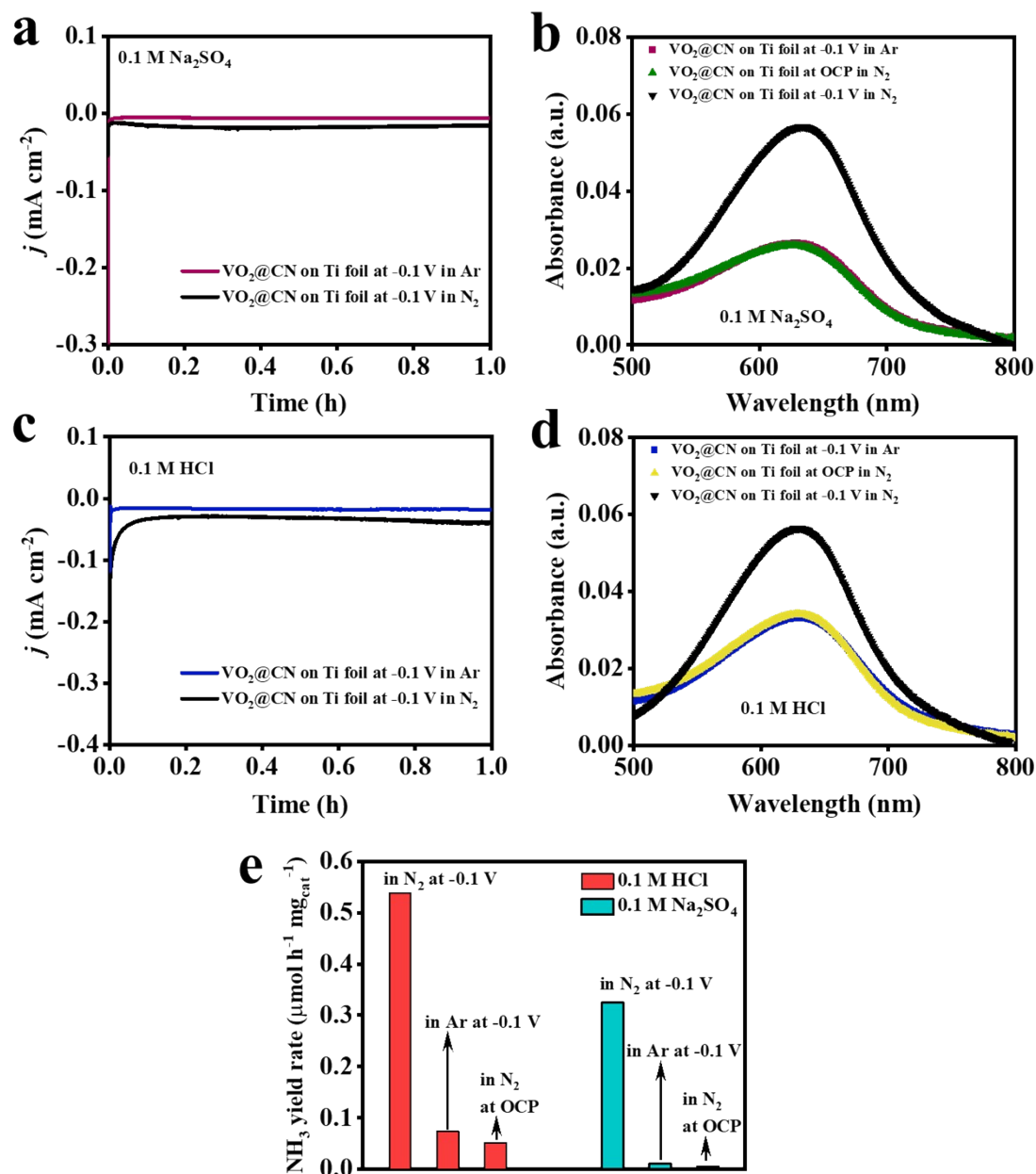


Figure S18. CA plots and corresponding UV-visible spectra of VO₂@CN catalyst in N₂ at -0.1 V, in Ar at -0.1 V and in N₂ at open circuit potential (OCP) in (a,b) 0.1 M Na₂SO₄ and (c,d) 0.1 M HCl; (e) represents the bar plot showing comparative NH₃ yield rate in all of the above mentioned conditions in both the electrolytes.

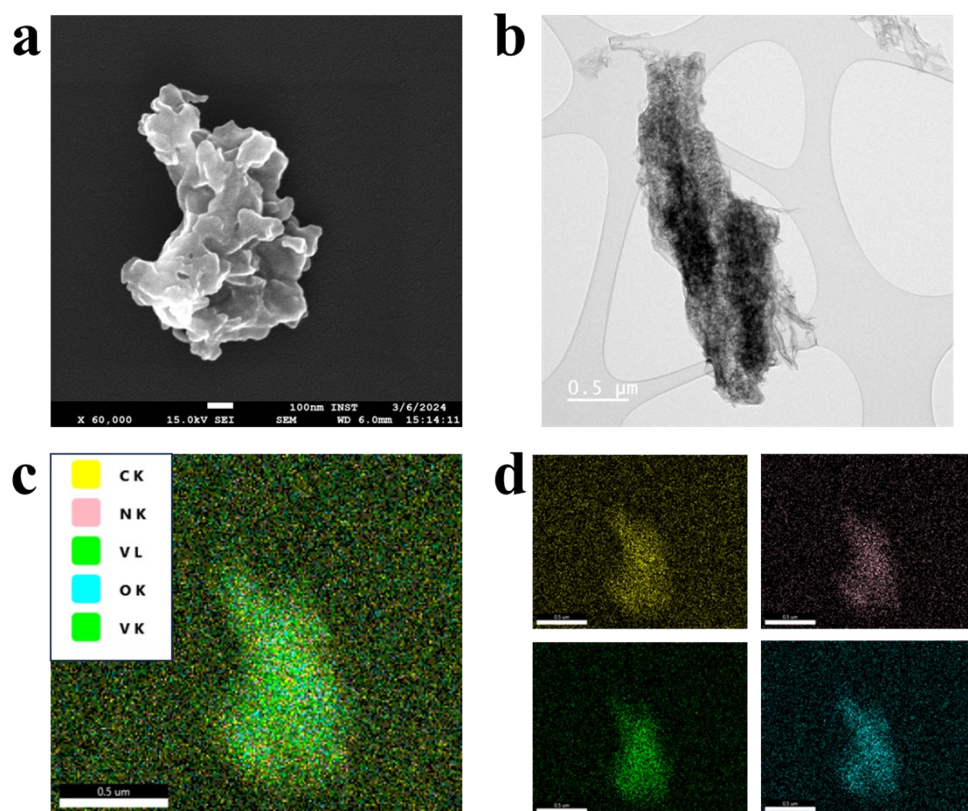


Figure S19. Post-stability morphological characterization of $\text{VO}_2@\text{CN}$ catalyst with (a) FESEM and (b) TEM imaging; (c, d) cumulative and individual elemental mapping of all the elements C, N, V and O of the after-stability sample.

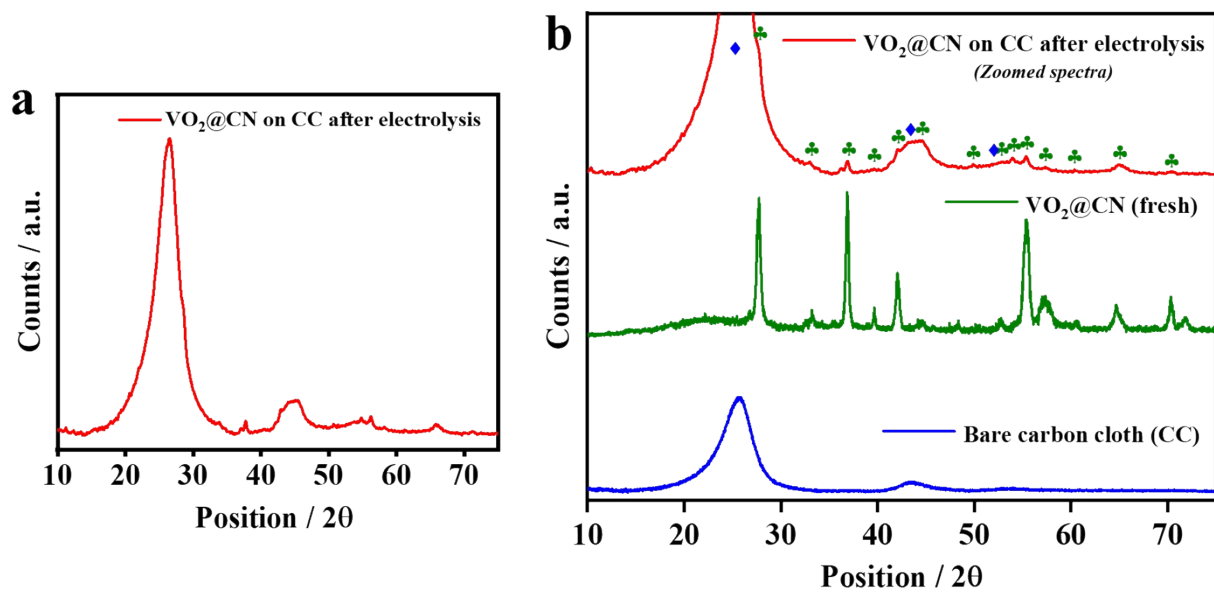


Figure S20. (a) Post-electrolysis XRD spectra of $\text{VO}_2@\text{CN}$ on carbon cloth and (b) zoomed spectra of $\text{VO}_2@\text{CN}$ sample on CC after electrolysis, compared with bare CC and fresh $\text{VO}_2@\text{CN}$ sample.